EMC Simulation of Complex PCB inside a Metallic Enclosure and Shielding Effectiveness Analysis

Antonio Ciccomancini Scogna [#], Martin Schauer[#]

[#]CST of America, Inc.
10 Laurel Avenue, Suite 300, Wellesley Hills, MA 02481USA
[1]antonio.ciccomancini@cst.com
[2]martin.schauer@cst.com

Abstract— **In the present paper the Finite Integration Technique (FIT) in combination with the Partial Element Equivalent Circuit (PEEC) is employed to investigate the shielding performance of a metallic enclosure used for digital switching equipment. The current distribution on the power plane of a complex printed circuit board is used to excite the system. The effect of apertures' shape and configuration on the value of the radiated Electric field is studied. It is shown that dividing a specified area into a combination of multiple apertures may reduce the value of the radiated emissions and therefore improve the shielding effectiveness. The usage of honeycomb panels is finally investigated.**

I. Introduction

In order to comply with the stringent radiated emission limits imposed by the standards and taking into account the increasing clock speed and data rates of current high-speed digital electronics, it is often necessary to shield the enclosure where the Printed Circuit Board (PCB) is located. A thorough EMC or Signal Integrity assessment of a complete board or system is often a daunting task due to the extreme complexity of modern electronic systems.

System designers would like to accurately evaluate the electromagnetic interference (EMI) produced by high-speed signals. This capability is useful in predicting and correcting interference problems at various stages in the design process. There are several requirements for an accurate evaluation of these effects. First, the complicated multilayered board and package structures used in today's designs, including signal traces, supply planes and vias, must be modeled in a way that takes into account full-wave effects.

Secondly, the behavior of various shielding structures such as metallic enclosures must be taken into account as well. Finally, the issue of problems consisting of small structures embedded in large computational domains must be addressed. Performing such analysis is often a computational challenge. A three dimensional (3D) solver is desirable for modeling the arbitrary shapes of the enclosures (which often includes slots, apertures [1]), but simulating a multi-layer board or package can be difficult and memory consuming.

The problem results from the high complexity of modern boards and packages and the 3D nature of the system enclosures surrounding them.

We address this problem by using the following approach: 1) a specialized Partial Element Equivalent Circuit (PEEC) [2] is employed to compute the current distribution on the power (PWR) plane of a complex PCB, 2) a full-wave Finite Integration Technique (FIT) [3] is used to analyze the shielding performance of a metallic enclosure due to the calculated current distribution.

The effect of apertures' shape and configuration on the value of the radiated Electric field and the related shielding effectiveness (SE) are studied. It is shown that dividing a specified area into a combination of multiple apertures may reduce the value of the radiated emissions. The usage of honeycomb panels is also investigated.

The structure of the paper is the following: in the next section the FIT technique is briefly described and validated by using as test vehicle a model already existent in literature [4]. In Section III the equivalent electromagnetic model used for the numerical simulation, the workflow process and the SE results are discussed. Finally Section IV draws some concluding remarks.

II. FIT Code Validation

The numerical technique used to characterize the full structure (board and metallic enclosure) is the FIT, first proposed by T. Weiland [5].

FIT falls in the class of differential time-domain methods and generates exact algebraic analogs to Maxwell's equations that guarantee physical properties of computed fields and lead to one solution. Maxwell's equations, and the related material equations, are transformed from the continuous domain into a discrete space by allocating electric voltages on the edges of a grid G and magnetic voltages on the edges of a dual grid $\tilde{G}$. The allocation of the voltage and flux components on the grid can be seen in Fig. 1.

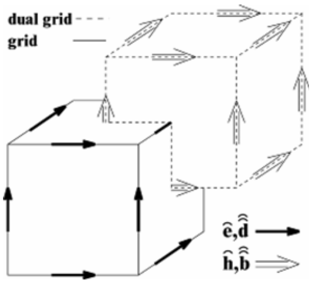

Fig. 1 Allocation of the electric and magnetic components in the spatial grids.

The discrete equivalent of Maxwell's equations, the so-called Maxwell's Grid Equations, are (1)–(4)

$$C\hat{e} = -\frac{d}{dt}\hat{\hat{b}} \quad (1)$$

$$\tilde{C}\hat{h} = \frac{d}{dt}\hat{\hat{d}} + \hat{\hat{j}} \quad (2)$$

$$S\hat{\hat{b}} = 0 \quad (3)$$

$$\tilde{S}\hat{\hat{d}} = q \quad (4)$$

In these equations, $\hat{e}$ and $\hat{h}$ denote the electric voltages between grid points and the magnetic voltages between dual grid points, respectively. The symbols $\hat{\hat{d}}$, $\hat{\hat{b}}$ and $\hat{\hat{j}}$ are fluxes over grid or dual-grid faces.

Due to the consistent transformation, analytical properties of the fields are maintained, resulting in corresponding discrete topological operators on the staggered grid duplet. The topology matrices, C, $\tilde{C}$, S and $\tilde{S}$ correspond to the curl and the div-operators. The tilde indicates that the operator belongs to the dual grid. The discrete analog of the coupling between voltages and fluxes is represented by the material matrices M_{ε}, $M_{\mu^{-1}}$ and M_{κ}.

$$\hat{\hat{d}} = M_{\varepsilon}\hat{e} \quad (5)$$

$$\hat{h} = M_{\mu^{-1}}\hat{\hat{b}} \quad (6)$$

$$\hat{\hat{j}} = M_{\kappa}\hat{e} + \hat{\hat{j}}_A \quad (7)$$

In all of the simulations performed in this paper, the conductive parts of the structures have been simulated as perfect electric conductive material (PEC), enforcing the tangential component of the electric field being zero.
Equations (1)–(4) along with (7)–(7) are solved in the time domain.

The discretization of the time derivative is formulated as an explicit algorithm in a way that the FIT in the time domain can be considered as a generalization of the Finite Difference Time Domain (FDTD) method. The transient waveforms obtained by the simulations are then converted in the frequency domain by a fast Fourier transform.

To check the reliability of the FIT-based code the enclosure model presented in [4] has been built: it is a rectangular box of size (30 x 12 x 30 in centimeters) with a rectangular aperture of size (10 x 0.5) located at the center of the frontal wall (15, 6, and 0).

The enclosure is illuminated by a normal incident plane wave (farfield source) at 0 degree polarization and three probes are placed in the center position inside the enclosure in order to register the three components of the electric field (Ex, Ey, Ez) and to calculate the SE afterwards.

Fig.2 plots the SE results of FIT, other numerical techniques as well as measurements. A good agreement can be observed over the considered frequency range.

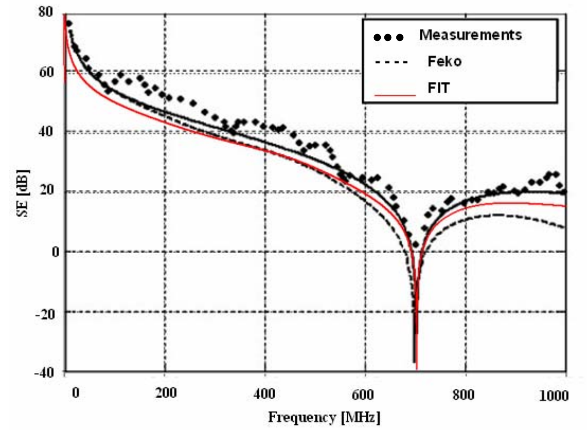

Fig. 2 SE versus frequency at the center of the enclosure illuminated by a normal incident plane wave.

III. 3D ELECTROMAGNETIC MODEL AND SIMULATION STRATEGY

A view of the metallic enclosure analyzed in the present paper is shown in Fig. 3a: it is a 370 x 90 x 296 mm box with a front panel with 2 rectangular apertures of dimensions: 126 x 14 mm and 80 x 60mm.

On the top of the box is mounted a cover, inside it there are two boards (see Fig.3b) and a heat sink.

The thickness of the metal walls (PEC) is t = 2 mm and the dielectric material of the board 1 has relative electric permittivity $\varepsilon_r = 4.0$.

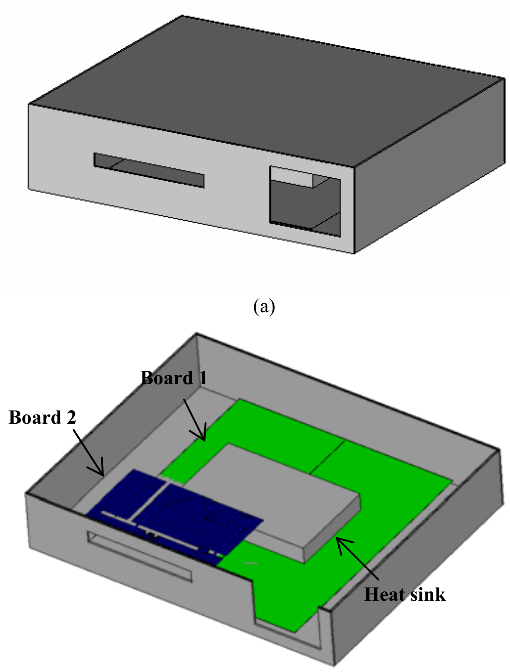

(b)

Fig. 3 Three dimensional (3D) view of the metallic enclosure.

Board 2 is a typical 6 layers PCB with hundred of nets, vias and connections. The PWR plane is split in islands by means of gaps. Due the complexity of the board, the dynamic link with a PEEC based code [2] is used to evaluate the current distribution on the PWR plane. The calculate field is then used within the FIT in order to perform the 3D numerical simulation of the metallic enclosure. The workflow design process is summarized in Fig.4.

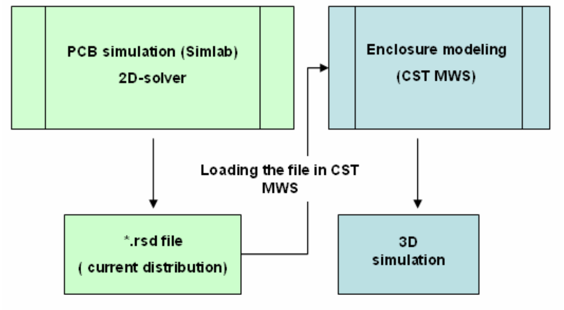

Fig. 4 Workflow process.

Electric field components are calculated in a specific location 3m distant from the frontal panel of the metallic box and the SE is also analyzed. In the considered frequency range the EM fields inside the enclosure are dominated by the first two waveguide modes and the orientation of the slots located in the frontal part of the enclosure is such that the vertical Electric field component can couple easily across the aperture.

The SE can be found from the ratio of the field strengths without and with the enclosure:

$$SE_E = 20\log\left|\frac{E_0}{E}\right| \tag{8}$$

Due to the highly resonant behavior of the box, in order to speed up the simulation time a very small value of loss is distributed throughout the solution space by artificially assigning a conductivity (σ=0.002 S/m) to the free space cells of the calculation domain. In [6-7] it has already demonstrated how this artifact has practically no influence of the far field calculated results.

In order to study the effect of the apertures located on the frontal panel, three different cases are analyzed, as illustrated in Fig.5. The SE value for the tree considered cases is reported in Fig.6

Important considerations can be addressed: 1) Case 1 shows possible problems when increasing the frequency and at 2GHz the SE reaches almost a negative value, 2) Case 2 doesn't offer a sensible improvement of the SE, 3) Case 3 is the only situation where the SE can be considered acceptable within the considered frequency range.

The reason of this last case is certainly related to the fact that for rectangular apertures varying the length to width ratio changes the location of the resonant frequency, therefore improving the SE.

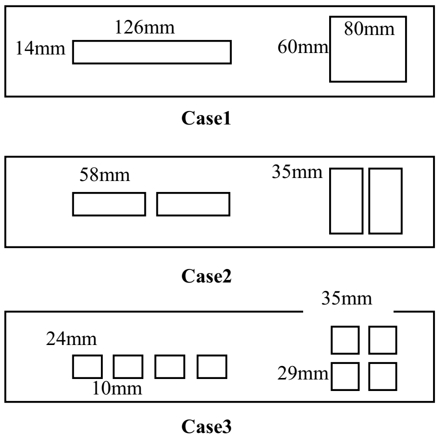

Fig. 5 Different apertures size of the frontal panel.

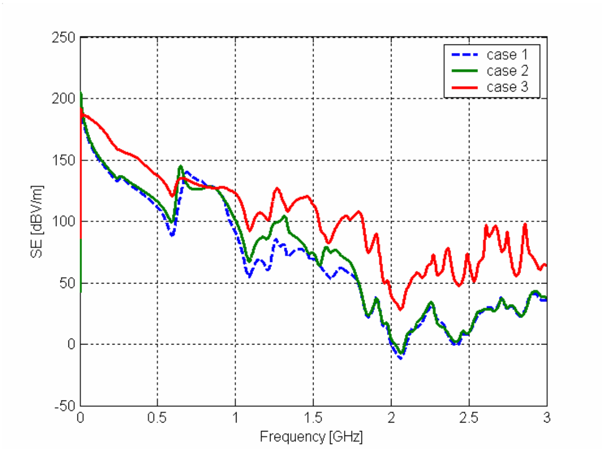

Fig. 6 Comparison of electric SE for the different configurations reported in Fig.1

Fig.7 (a-b) depicts the Electric field, calculated at 2GHz for Case 1 and Case 3 and it straightforward to note how the electromagnetic waves are coming out the metallic enclosure thought the single apertures (a), while they are somehow contained within the enclosure in the Case 3 (b).

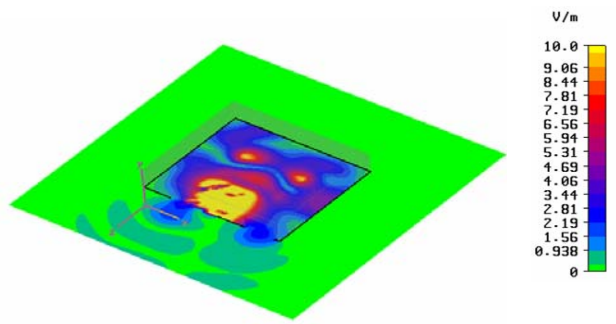

Fig. 7a Electric field at 2GHz for the case 1.

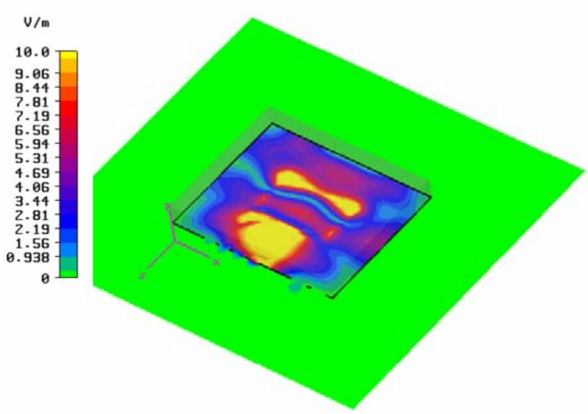

Fig. 7b Electric field at 2GHz for the case 3.

At this point the apertures located in the frontal panel of the metallic enclosure are covered by means of honeycomb panels, according to Fig.8.

For the left panel circular holes of 2mm diameter, 1mm distant each other are employed, while for the right panel circular holes of 4mm diameter and 2mm distant each other are modelled. The calculated results are reported in Fig. 9 where the comparison with case 1 is presented.

A sensible improvement (of more than 100dB) can be observed in this case, which shows the high performance of honeycomb panels.

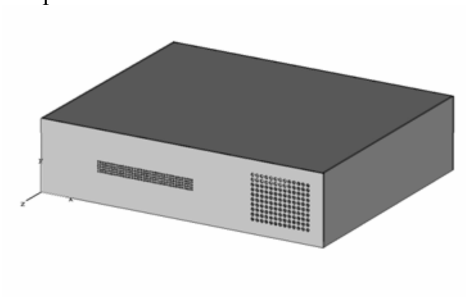

Fig. 8 3D view of the metallic enclosure with honeycomb panels.

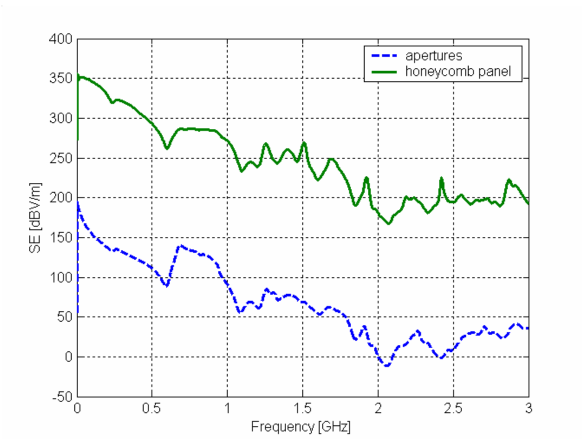

Fig. 9 SE: comparison between Case 1 and honeycomb panel.

IV. Conclusions

The effect of different shapes and configuration of apertures on the SE of a metallic enclosure is studied. By combining a specialized board analysis tools based on PEEC method with a 3D full wave simulation tool (FIT), we have demonstrated an approach to computing the electromagnetic emissions of complex electronic systems, including multilayered packages, printed circuit boards, and complicated metallic enclosures.

The proposed workflow consists on three steps: 1) simulation of the complex PCB, 2) surface current distribution used to excite the enclosure and 3) full wave simulation of the metallic box.

The SE of some combinations of multiple apertures is investigated and it is shown that dividing a fixed area into some smaller apertures will lead to more efficient shielding than implementing only one aperture. This is helpful when optimizing the shape of open area used to feed trough cables or heat dissipation. The SE when honeycomb panels are employed is also analyzed.

Acknowledgment

The authors wish to thank Simlab GmbH and Mr. F. Zanella for providing the RSD file used within CST MWS for the full wave numerical simulation.

References

[1] V. Rajamani, C. Bunting, M. D. Deshpande, Z. A. Khan, "Validation of modal/MoM in shielding effectiveness studies of rectangular enclosures with apertures", *IEEE Trans. Electromagn. Compat*ibility, vol. 48, no. 2, May 2006, pp. 348-353.

[2] PCBmod, Simlab – also available online at www.simlab.com

[3] CST Studio Suite 2006B – also available online at www.cst.com

[4] C. F. Bunting, Khan Z. A. and Deshpande, M.D, "Shielding effectiveness of metallic enclosures at oblique and arbitrary polarizations" *IEEE Trans. Electromagn. Compat*., vol. 47, no. 1, Feb. 2005, pp. 112–122.

[5] T. Weiland, "A Discretization Method for the Solution of Maxwell's Equation for Six Component Fields", *Electronics and communication*, (AEÜ), Vol.31, (1977)

[6] G. Antonini, A.Ciccomancini Scogna, A.Orlandi, "Shielding analysis of a metallic enclosure by means of a statistical approach" in *Proceedings of EMC Europe 04*, Eindhoven, 6-10 September, 2004.

[7] A. Ciccomancini Scogna, "Shielding Performance of a Metallic Rack used for Telecommunication Equipments: FIT modeling and Measurements", in *Proceedings of IEEE Int. Symposium on EMC Zurich 06,* Singapore, February 2006.

射 频 和 天 线 设 计 培 训 课 程 推 荐

易迪拓培训(www.edatop.com)由数名来自于研发第一线的资深工程师发起成立，致力并专注于微波、射频、天线设计研发人才的培养；我们于 2006 年整合合并微波 EDA 网(www.mweda.com)，现已发展成为国内最大的微波射频和天线设计人才培养基地，成功推出多套微波射频以及天线设计经典培训课程和 ADS、HFSS 等专业软件使用培训课程，广受客户好评；并先后与人民邮电出版社、电子工业出版社合作出版了多本专业图书，帮助数万名工程师提升了专业技术能力。客户遍布中兴通讯、研通高频、埃威航电、国人通信等多家国内知名公司，以及台湾工业技术研究院、永业科技、全一电子等多家台湾地区企业。

易迪拓培训课程列表：http://www.edatop.com/peixun/rfe/129.html

射频工程师养成培训课程套装

该套装精选了射频专业基础培训课程、射频仿真设计培训课程和射频电路测量培训课程三个类别共 30 门视频培训课程和 3 本图书教材；旨在引领学员全面学习一个射频工程师需要熟悉、理解和掌握的专业知识和研发设计能力。通过套装的学习，能够让学员完全达到和胜任一个合格的射频工程师的要求…

课程网址：http://www.edatop.com/peixun/rfe/110.html

ADS 学习培训课程套装

该套装是迄今国内最全面、最权威的 ADS 培训教程，共包含 10 门 ADS 学习培训课程。课程是由具有多年 ADS 使用经验的微波射频与通信系统设计领域资深专家讲解，并多结合设计实例，由浅入深、详细而又全面地讲解了 ADS 在微波射频电路设计、通信系统设计和电磁仿真设计方面的内容。能让您在最短的时间内学会使用 ADS，迅速提升个人技术能力，把 ADS 真正应用到实际研发工作中去，成为 ADS 设计专家...

课程网址： http://www.edatop.com/peixun/ads/13.html

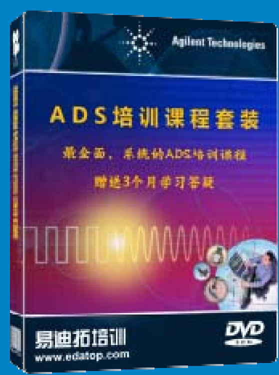

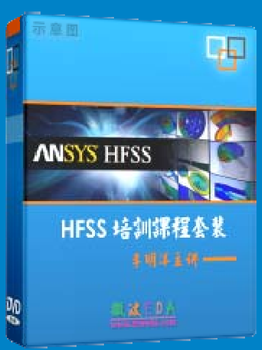

HFSS 学习培训课程套装

该套课程套装包含了本站全部 HFSS 培训课程，是迄今国内最全面、最专业的 HFSS 培训教程套装，可以帮助您从零开始，全面深入学习 HFSS 的各项功能和在多个方面的工程应用。购买套装，更可超值赠送 3 个月免费学习答疑，随时解答您学习过程中遇到的棘手问题，让您的 HFSS 学习更加轻松顺畅…

课程网址：http://www.edatop.com/peixun/hfss/11.html

CST 学习培训课程套装

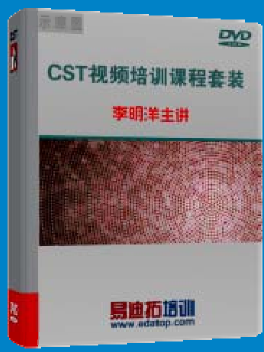

该培训套装由易迪拓培训联合微波 EDA 网共同推出，是最全面、系统、专业的 CST 微波工作室培训课程套装，所有课程都由经验丰富的专家授课，视频教学，可以帮助您从零开始，全面系统地学习 CST 微波工作的各项功能及其在微波射频、天线设计等领域的设计应用。且购买该套装，还可超值赠送 3 个月免费学习答疑…

课程网址：http://www.edatop.com/peixun/cst/24.html

HFSS 天线设计培训课程套装

套装包含 6 门视频课程和 1 本图书，课程从基础讲起，内容由浅入深，理论介绍和实际操作讲解相结合，全面系统的讲解了 HFSS 天线设计的全过程。是国内最全面、最专业的 HFSS 天线设计课程，可以帮助您快速学习掌握如何使用 HFSS 设计天线，让天线设计不再难…

课程网址：http://www.edatop.com/peixun/hfss/122.html

13.56MHz NFC/RFID 线圈天线设计培训课程套装

套装包含 4 门视频培训课程，培训将 13.56MHz 线圈天线设计原理和仿真设计实践相结合，全面系统地讲解了 13.56MHz 线圈天线的工作原理、设计方法、设计考量以及使用 HFSS 和 CST 仿真分析线圈天线的具体操作，同时还介绍了 13.56MHz 线圈天线匹配电路的设计和调试。通过该套课程的学习，可以帮助您快速学习掌握 13.56MHz 线圈天线及其匹配电路的原理、设计和调试…

详情浏览：http://www.edatop.com/peixun/antenna/116.html

我们的课程优势：

※ 成立于 2004 年，10 多年丰富的行业经验，

※ 一直致力并专注于微波射频和天线设计工程师的培养，更了解该行业对人才的要求

※ 经验丰富的一线资深工程师讲授，结合实际工程案例，直观、实用、易学

联系我们：

※ 易迪拓培训官网：http://www.edatop.com

※ 微波 EDA 网：http://www.mweda.com

※ 官方淘宝店：http://shop36920890.taobao.com